

Design and Prototyping of Transmissive RIS-Aided Wireless Communication

Jianan zhang¹, Rujing Xiong¹, Junshuo Liu¹, Tiebin Mi¹, Robert Caiming Qiu¹

¹School of Electronic Information and Communications, Huazhong University of Science and Technology, Wuhan 430074, China
Emails: {zhangjn, rujing, junshuo_liu, mitiebin, caiming}@hust.edu.cn

Abstract—Reconfigurable Intelligent Surfaces (RISs) exhibit promising enhancements in coverage and data rates for wireless communication systems, particularly in the context of 5G and beyond. This paper introduces a novel approach by focusing on the design and prototyping of a transmissive RIS, contrasting with existing research predominantly centered on reflective RIS. The achievement of 1-bit transmissive RIS through the anti-symmetry configuration of the two PIN diodes, nearly uniform transmission magnitudes but inversed phase states in a wide band can be obtained. A transmissive RIS prototype consisting of 16×16 elements is meticulously designed, fabricated, and subjected to measurement to validate the proposed design. The results demonstrate that the proposed RIS unit cell achieves effective 1-bit phase tuning with minimal insertion loss and a transmission bandwidth of 3 dB exceeding 20% at 5.8GHz. By dynamically modulating the quantized code distributions on the RIS, it becomes possible to construct scanning beams. The experimental outcomes of the RIS-assisted communication system validate that, in comparison to scenarios without RIS, the signal receiving power experiences an increase of approximately 7dB when RIS is deployed to overcome obstacles. This underscores the potential applicability of mobile RIS in practical communication.

Index Terms—Transmissive RIS, prototype, phase shift, beam-forming

I. INTRODUCTION

RECONFIGURABLE Intelligent Surfaces (RISs) have attracted significant interest in the recent years from both academia and industry [1] [2]. Recently, RIS has attracted great attention for its capability of making full use of spatial resources and improving spectral efficiency by smartly manipulating electromagnetic (EM) environments [3]. Practically speaking, an RIS can be built using artificial electromagnetic metamaterial, which consists of periodic arrangements of specifically designed subwavelength-sized structural elements [4]. Such metamaterials have unique electromagnetic properties that do not exist in nature [5], such as, negative refraction [6], perfect absorption, and anomalous reflection/scattering. The intelligent reconfiguration of the phase states of RIS elements enables the formation of arbitrary beam shapes at a relatively low cost and power consumption. RIS technology offers substantial advantages in extending network coverage, enhancing capacity, conserving power, and mitigating interference in beyond 5G (B5G) networks. Consequently, numerous signal processing techniques and experimental studies have been conducted to showcase the efficacy of RIS technology [7] [8].

However, current research efforts predominantly focus on the application of reflective Reconfigurable Intelligent Surfaces (RIS) [7] [8] [9] [10]. This emphasis on reflective RIS poses the risk of creating undesirable coverage gaps within cellular networks, ultimately limiting the overall applicability of RIS technology. Notably, reflective RIS introduces a constraint where both the base station and user must be situated on the same side of the RIS, imposing additional geographical restrictions on the network's physical topology [11]. For instance, facilitating communication between a transmitter outside a vehicle and a receiver inside it becomes challenging with reflective RIS. To address these limitations and broaden the scope of RIS applications, increasing attention is being directed toward the concept of transmissive RIS [12]. In contrast to reflective RIS, where signals are reflected, transmissive RIS enables signals to pass through, forming directional beams. This unique characteristic of transmissive RIS holds the potential to effectively fill the coverage gaps left by reflective RIS, overcoming challenges associated with constrained communication scenarios. The rising interest in transmissive RIS underscores its significance in mitigating limitations associated with reflective RIS and expanding the application possibilities within wireless communication networks.

The phase reconfigurability is the most essential capability for a transmissive RIS. Solid-state electronic devices are commonly integrated in each constituent RIS element to dynamically control its phase response. Continuous phase shifts can be realized using analog-type devices like varactor diodes, PIN diodes, Micro-Electro-Mechanical System, and etc (MEMS) switches [13] [14] [15] [16] [17].

In this paper, an efficient transmissive metasurface is presented to generate dynamically scanning beams. The designed metasurface unit can provide very high transmission efficiency, and the 1-bit phase tuning of the unit is obtained by integrating two PIN diodes in the unit structure for current inversion. Through the modulation of the switchable status on PIN diodes by using programmable bias circuit, dynamical scanning beams can be created. The simulation and experimental results verify the effectiveness of the proposed design. Finally, the transmitted RIS is integrated into the wireless communication system, which shows good capability in the scenario of through-the-wall. The main contributions of our work are as follows:

TABLE I
PARAMETERS FOR THE TRANSMISSIVE UNIT CELL IN MILLIMETERS

Parameter	L	L_p	W_p	H_1	H_2	W_s	t	d_1	d_2
Value	18	15	11	2	2	8	2	0.3	0.5

- The achievement of 1-bit transmissive RIS through the antisymmetry configuration of the two PIN diodes, nearly uniform transmission magnitudes but inversed phase states in a wide band can be obtained.
- Furthermore, a prototype with 16×16 RIS elements and a logic circuit control board is fabricated and measured. The measured results show that the prototype can achieve 180° phase shift. Moreover, the measured radiation performances for scan angles are presented as well, demonstrating the beamsteering capability.
- Finally, a transmissive RIS-aided wireless communication prototype is developed to demonstrate the performance in the scenario of through-the-wall. The experimental results verify that transmitted RIS enhanced the gain by about 7dB.

The rest of this paper is organized as follows. Section II describes the structure and simulated performance of the element of the designed transmissive RIS. Section III provides the experimental results for the 16×16 elements RIS prototype.

II. RIS DESIGN

A. unit cell design

The geometry of the RIS unit-cell is shown in Fig. 1, which is made up of four copper layers supported by three substrate layers. The copper layers encompass, from top to down, the radiating layer, the ground plane, the receiving layer, and the bias layer. The radiating layer is composed of a rectangular annular patch and a rectangular patch with two PIN diodes (#1 and #2) integrated at the junctions along the x -axis. The outer rectangular annular patch is connected with the ground plane by two metallized via-holes symmetrically on the horizontal center line through the receiving layer, while the rectangular inner patch is connected with the receiving layer by a metallized via-hole at the center through the ground, which consists of the same size rectangular annular patch loaded by a U-slot. Besides, the receiving layer is also connected with the bias layer through center metallized via-holes for biasing purposes, and the bias layer is integrated with a 15 nH inductor to isolate the high frequency signals from the patches to the bias lines. The substrate 1 and substrate 2 layers are designed using a F4B ($\epsilon_r = 3.5$, $\tan \delta = 0.001$, $H_1, H_2 = 2\text{mm}$), while the bias layer is with a dielectric substrate 3 ($\epsilon_r = 4.3$, $\tan \delta = 0.025$, $H_1, H_2 = 0.2\text{mm}$). The detailed dimensions of the proposed unit are also provided in table I.

The two PIN diodes integrated on the unit are placed with antisymmetry configuration as shown in Fig 1(b), resulting in the opposite PIN biased states for any of the two operation states. When PIN diode #1 is switched off and PIN diode #2 switched on, the proposed reconfigurable unit is operating at the 0-state. Correspondingly, the 1-state can be acquired

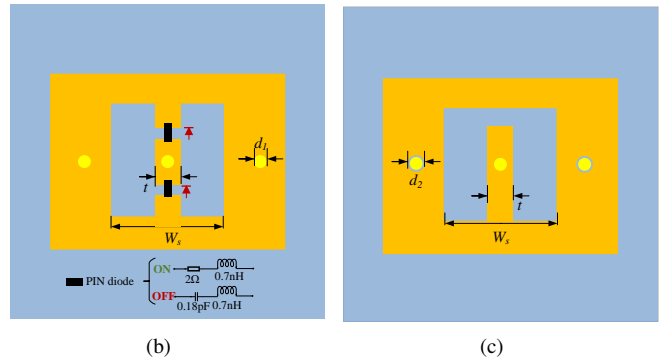
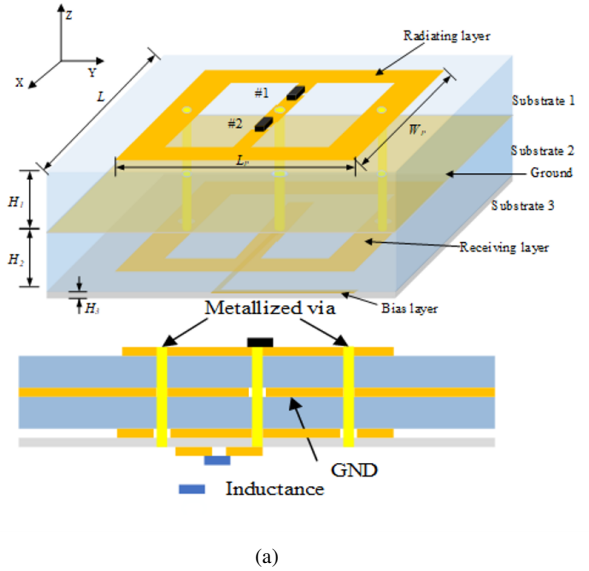


Fig. 1. Geometry of the designed metasurface element, (a) schematic and side view, (b) Radiating layer and (c) Receiving layer

with PIN diode #1 switched on and PIN diode #2 switched off. Fig. 2 depicts the induced current distribution on the radiating layer and receiving layer in two states. Since the current directions of the receiving layer in 0-state and 1-state are opposite, a phase shift of transmitted wave on the unit cell can be obtained between two cases. That is, the two coaxial patches on the radiating layer would be concatenated at the upper or nether junction for the two coding states, respectively, leading to a current inversion for the two operation coding states and obtaining the inverting transmission coefficients with nearly uniform magnitudes but inversed phase states in a wide frequency band. The PIN diode SMP1345-079LF is adopted to acquire lower unit insertion losses within the designed frequency band, which is modeled by the lumped components in series for ON/OFF states, respectively. For the ON state with a forward dc-biasing voltage, a series of lumped resistance ($R = 2 \Omega$) and inductance ($L = 0.7 \text{ pH}$) is adopted for the PIN diode; while for the OFF state with a reverse dc-biasing voltage, a capacitance ($C = 0.18 \text{ pF}$) and inductance ($L = 0.7 \text{ pH}$) is employed. The specific equivalent circuits are

shown in Fig. 1(b).

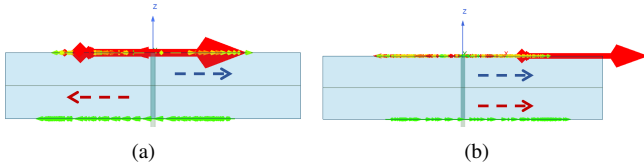


Fig. 2. Current distribution on the unit cell, (a) 0-state, (b) 1-state

The electromagnetic simulation of the proposed transmissive unit is carried out with help of the commercial software package CST Microwave Studio by using unit cell boundary conditions along with Floquet-port excitations. The simulated scattering coefficients with both magnitude and phase for the two phase states of the unit cell are shown in Fig. 3. When the proposed unit is operating at the 0-state and 1-state, the S_{21} at 5.4 GHz to 6.6 GHz is greater than -3 dB. The simulated 3 dB transmission bandwidths are over 20%, with the minimum insertion losses of only 0.5 dB at 5.8 GHz. It is worth mentioning that the phase curves of the two coding cases are basically parallel throughout the frequency band, and the phase difference is about 180° .

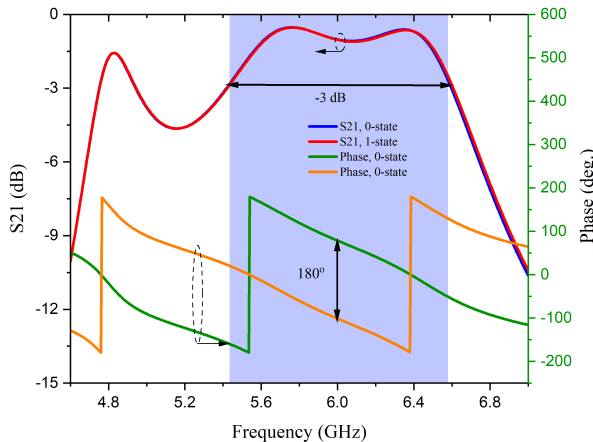


Fig. 3. Simulated results of unit-cell in different states

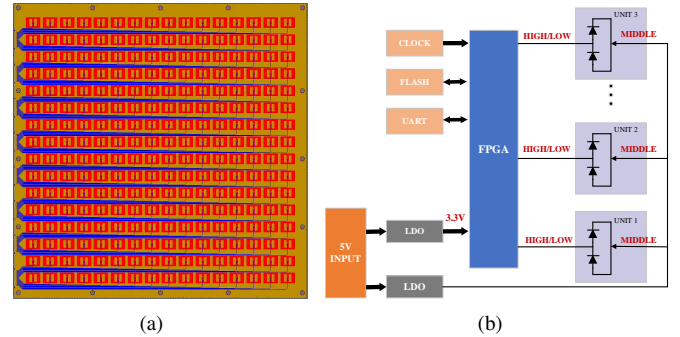
B. Array design and fabrication

In this section, a transmissive RIS prototype composed of 16×16 proposed unit cells is designed, fabricated, and measured to experimentally validate the performance of the proposed RIS unit cell, where the bias lines should be arranged on the upper and lower edges of the unit cell and minimize the bias-layer interference, as shown in 4(a).

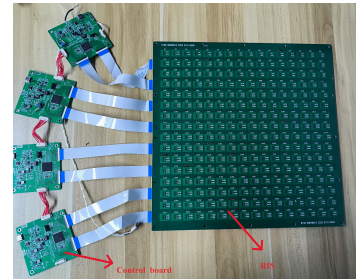
The transmissive RIS encompasses a total of 512 PIN diodes and the state of each unit cell is modulated through the bias layer network, which are interfaced to eight 1×34 pins connectors. The steering-logic board is also designed and fabricated, and the schematic diagram of the circuit design is shown in Fig. 4. The whole control system is powered

by a voltage input supply (5 V), and an extra low dropout regulator (LDO) provides an external reference voltage for the metasurface ground plane (marked as MIDDLE). with an overall dimension of $300 \times 300 \text{ mm}^2$.

The photographs of the fabricated RIS prototype are presented in Fig. 4(c). Taking advantage of the PCB technology, the RIS is easy to fabricate. To achieve the goal of phase reconfigurability, each element of the array needs to be controlled independently. There are 256 biasing lines since each element has one biasing lines to apply DC voltages to two PIN diodes. Four logic circuit controlling boards are attached to supply independent DC voltages.



(a) (b)



(c)

Fig. 4. a) The bias layer network layout. b) Schematic diagram of the steering logic board circuit design. (c) the fabricated transmissive RIS prototype.

III. EXPERIMENTAL RESULTS

In this section, we present the results from several experiments that were made using our prototype to verify the performance of this proof-of-concept. First, we test the electromagnetic transmission coefficients of the RIS. Next We test the radiation pattern in an anechoic chamber to measure the beamforming function of RIS. Finally, RIS is embedded into the wireless communication system to test its through-wall ability.

A. Transmission Coefficients

To evaluate the accuracy of the array design simulations, we measure the transmission coefficient (S_{21}) of RIS for both states using a vector network analyzer (VNA). As shown in Fig. 5, two antennas are placed on both sides of RIS 0.5 m away from the RIS and a sinusoidal signal at 5.8 GHz is used for the excitation. As plotted in Fig. 6, the experimental results show that the amplitude is -3 dB and the phase difference

is around 183° for a wide frequency range around 5.8 GHz which is in accordance to the simulations. The amplitude is also normalized and the maximum value is 0 dB.

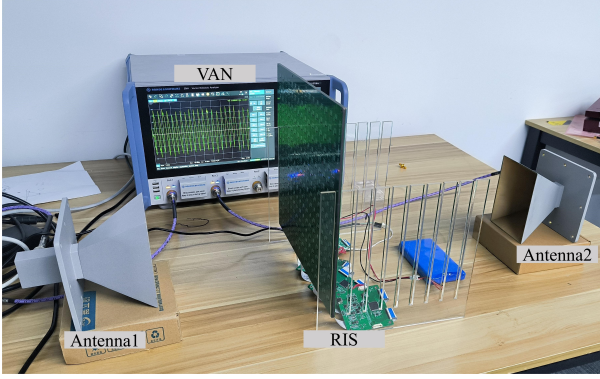


Fig. 5. S21 test environment

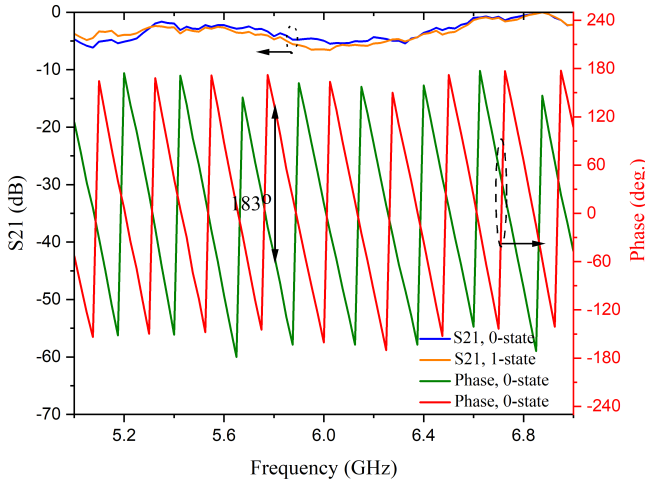


Fig. 6. Measured S21 of RIS for both states

B. Beamforming Performance

Next, we test the beamforming performance of the fabricated RIS. The experiment is carried out in a microwave anechoic chamber as shown in Fig. 7. The RIS is space-fed by a linearly polarized horn with an optimized distance of 260 mm. To stimulate the scanning beams codebooks through the transmissive metasurface, the theoretical phase compensation ϕ of each unit should satisfy the following equation [18].

$$\phi(x_i, y_i) = \frac{2\pi}{\lambda} (d_i - \sin \theta_0 (x_i \cos \varphi_0 + y_i \sin \varphi_0)). \quad (1)$$

where λ is the free-space wavelength at 5.8 GHz, (x_i, y_i) is the position of each element, (θ_0, φ_0) is the main beam direction, and d_i is the distance from the feed phase center to the i^{th} element. Three scanning beams along the axis direction are created as validations through the transmissive programmable metasurface. The result is shown in Fig. 8, the measured scanned beams in the angular 0° , 10° and 45° show accurate beam pointing and well-defined patterns.



Fig. 7. The measurement setup in the microwave anechoic chamber.

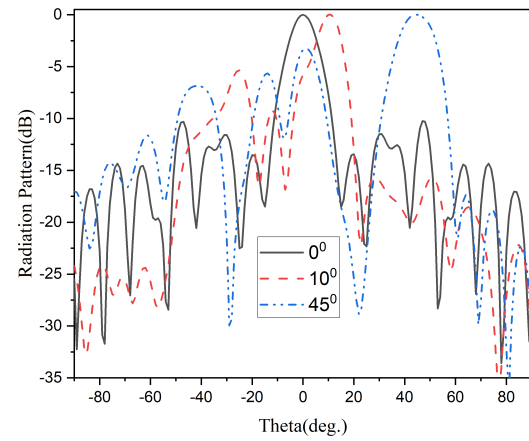


Fig. 8. Measured radiation patterns of scanned beams at 5.8 GHz

C. Through-wall experiment

In this section, a transmissive RIS-aided wireless communication prototype is set up to further measure the performance of the designed transmissive RIS in practical communication scenarios.

To assess the efficacy of RIS in overcoming obstacles, we conduct experiments within an office setting, depicted in Figure 9. The prototype comprises the transmitter side, the RIS, and the receiver side. Both the transmitter and the receiver employ the software-defined radio (SDR) platform. The transmitter is situated within the office, while the receiver is positioned in the corridor with a 30 mm concrete barrier between them, and the RIS positioned against the wall. Let d_1 denote the distance between the Tx antenna and the RIS, and Table II shows the receiving power at different d_1 . When d_1 is 0.5m, 0.8 m and 1.65m respectively, the gain of with RIS is 8dBm, 7dBm and 6dBm higher than that of without RIS. The experimental results show that RIS has a good performance in penetrating obstacles.

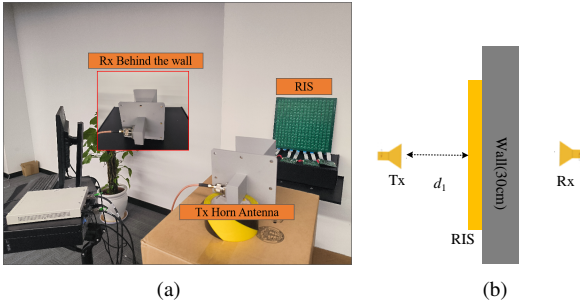


Fig. 9. Transmissive RIS-aided wireless communication prototype, (a) Experimental scene, (b) schematic diagram.

TABLE II
RECEIVING POWER WITH OR WITHOUT RIS UNDER DIFFERENT d_1

d_1	0.5 m	0.8 m	1.65 m
Received power(without RIS)	-72 dBm	-72 dBm	-67 dBm
Received power(with RIS)	-64 dBm	-65 dBm	-61 dBm
Gain	8 dBm	7 dBm	6 dBm

IV. CONCLUSION

This work introduces an innovative 1-bit transmissive RIS through the antisymmetry configuration of the two PIN diodes, nearly uniform transmission magnitudes but inversed phase states in a wide band can be obtained. Experimental findings reveal that the transmissive RIS prototype with 16×16 unit cells, achieves a 180° phase shift and scanning beam at 5.8 GHz. Furthermore, a transmissive RIS-aided communication prototype is established, and its has a good performance in penetrating obstacles.

ACKNOWLEDGMENT

This work was supported in part by the Nation Natural Science Foundation of China under Grant No.12141107, and in part by the Interdisciplinary Research Program of HUST, 2023JCYJ012.

REFERENCES

- [1] C. Liaskos, S. Nie, A. Tsiolaridou, A. Pitsillides, S. Ioannidis, and I. Akyildiz, "A new wireless communication paradigm through software-controlled metasurfaces," *IEEE Communications Magazine*, vol. 56, no. 9, pp. 162–169, 2018.
- [2] E. Basar, M. Di Renzo, J. De Rosny, M. Debbah, M.-S. Alouini, and R. Zhang, "Wireless communications through reconfigurable intelligent surfaces," *IEEE access*, vol. 7, pp. 116753–116773, 2019.
- [3] W. Tang, M. Z. Chen, X. Chen, J. Y. Dai, Y. Han, M. Di Renzo, Y. Zeng, S. Jin, Q. Cheng, and T. J. Cui, "Wireless communications with reconfigurable intelligent surface: Path loss modeling and experimental measurement," *IEEE Transactions on Wireless Communications*, vol. 20, no. 1, pp. 421–439, 2020.
- [4] T. Cui, D. R. Smith, and R. Liu, "Metamaterials: Theory, design, and applications," *Springer Publishing Company, Incorporated*, 2009.
- [5] T. J. Cui, S. Liu, and L. Zhang, "Information metamaterials and metasurfaces," *Journal of materials chemistry C*, vol. 5, no. 15, pp. 3644–3668, 2017.
- [6] R. A. Shelby, D. R. Smith, and S. Schultz, "Experimental verification of a negative index of refraction," *science*, vol. 292, no. 5514, pp. 77–79, 2001.
- [7] L. Dai, B. Wang, M. Wang, X. Yang, J. Tan, S. Bi, S. Xu, F. Yang, Z. Chen, M. Di Renzo *et al.*, "Reconfigurable intelligent surface-based wireless communications: Antenna design, prototyping, and experimental results," *IEEE access*, vol. 8, pp. 45913–45923, 2020.

- [8] C. Huang, A. Zappone, G. C. Alexandropoulos, M. Debbah, and C. Yuen, "Reconfigurable intelligent surfaces for energy efficiency in wireless communication," *IEEE transactions on wireless communications*, vol. 18, no. 8, pp. 4157–4170, 2019.
- [9] X. Pei, H. Yin, L. Tan, L. Cao, Z. Li, K. Wang, K. Zhang, and E. Björnson, "Ris-aided wireless communications: Prototyping, adaptive beamforming, and indoor/outdoor field trials," *IEEE Transactions on Communications*, vol. 69, no. 12, pp. 8627–8640, 2021.
- [10] G. C. Trichopoulos, P. Theofanopoulos, B. Kashyap, A. Shekhawat, A. Modi, T. Osman, S. Kumar, A. Sengar, A. Chang, and A. Alkhateeb, "Design and evaluation of reconfigurable intelligent surfaces in real-world environment," *IEEE Open Journal of the Communications Society*, vol. 3, pp. 462–474, 2022.
- [11] Y. Wang, G. Wang, R. He, B. Ai, and C. Tellambura, "Doppler shift and channel estimation for intelligent transparent surface assisted communication systems on high-speed railways," *IEEE Transactions on Communications*, 2023.
- [12] N. DOCOMO, "Docomo conducts world's first successful trial of transparent dynamic metasurface (2020)."
- [13] M. Sazegar, Y. Zheng, C. Kohler, H. Maune, M. Nikfalazar, J. R. Binder, and R. Jakoby, "Beam steering transmitarray using tunable frequency selective surface with integrated ferroelectric varactors," *IEEE Transactions on Antennas and Propagation*, vol. 60, no. 12, pp. 5690–5699, 2012.
- [14] C. Huang, W. Pan, X. Ma, B. Zhao, J. Cui, and X. Luo, "Using reconfigurable transmitarray to achieve beam-steering and polarization manipulation applications," *IEEE Transactions on Antennas and Propagation*, vol. 63, no. 11, pp. 4801–4810, 2015.
- [15] A. Clemente, L. Dussopt, R. Sauleau, P. Potier, and P. Pouliguen, "1-bit reconfigurable unit cell based on pin diodes for transmit-array applications in x -band," *IEEE Transactions on Antennas and Propagation*, vol. 60, no. 5, pp. 2260–2269, 2012.
- [16] L. Di Palma, A. Clemente, L. Dussopt, R. Sauleau, P. Potier, and P. Pouliguen, "Circularly-polarized reconfigurable transmitarray in k -band with beam scanning and polarization switching capabilities," *IEEE transactions on antennas and propagation*, vol. 65, no. 2, pp. 529–540, 2016.
- [17] B. D. Nguyen and C. Pichot, "Unit-cell loaded with pin diodes for 1-bit linearly polarized reconfigurable transmitarrays," *IEEE Antennas and Wireless Propagation Letters*, vol. 18, no. 1, pp. 98–102, 2018.
- [18] P. Nayeri, F. Yang, and A. Z. Elsherbeni, "Reflectarray antennas: theory, designs, and applications," 2018.